THERMALLY STIMULATED INTERACTIONS IN BILAYERS AND MULTILAYERS CONTAINING Ni AND Si DURING A TEMPERATURE RAMP

A. Cvelbar, P. Panjan, B. Navinšek, B. Zorko and M. Budnar
"Jožef Stefan" Institute, Ljubljana, Slovenija

A.Zalar and B.Praček
Institute for Electronics and Vacuum Technique, Ljubljana, Slovenija

Keywords: silicides, silicide layers, microelectronics applications, thin films, bilayers, multilayers, Ni layers, Si layers, layer interactions, thermally stimulated interactions, dependability of layers thickness ratio, bilayer structures, multilayer structures, constant rate heating, temperature ramps, electrical resistivity, electrical resistivity measurement, XRD, x-ray diffraction, Seeman-Bohlin x-ray diffraction, Bragg-Bretano x-ray diffraction, Rutherford backscattering, RBS, Rutheford Backscattering Spectra, Auger Electron Spectroscopy depth profiling, Ni-Si overall stoichiometry, interdiffusion phases, oxygen contamination

Abstract: Interactions between Ni and Si films in different types of bilayers and multilayers during constant heating rate of 3 °C/min in Ar or N as a function of starting Ni and Si thicknesses with overall stoichiometry ranging from $Ni_{0.78}Si_{0.22}$ to $Ni_{0.28}Si_{0.72}$ was systematically studied by in-situ electrical resistivity, x-ray diffraction, Rutherford backscattering and Auger depth profiling up to 500 °C. Two different phase sequences observed depend on initial Ni/Si thickness ratio. Diffusion in multilayers is detected above 150 °C. Additionally, bilayers contaminated with different oxygen contents during deposition were analyzed during heating. Several per cent of incorporated oxygen in either Ni or Si layer suppresses the interdiffusion strongly.

Toplotno vzpodbujene interakcije v dvoplastnih in večplastnih zgradbah, vsebujočih nikelj in silicij med enakomernim segrevanjem

Ključne besede: silicidi, plasti silicidne, uporaba v mikroelektroniki, plasti tanke, dvoplasti, večplasti, Ni plasti niklja, Si plasti silicija, vplivi med plastmi, interakcije toplotno vzpodbujene, odvisnost od razmerja debelih plasti, strukture dvoplastne, strukture večplastne, segrevanje enakomerno, klančine temperaturne, upornost električna, merjenje upornosti električne, XRD uklon Rentgen žarkov, Seeman-Bohlin XRD uklon Rentgen žarkov, Bragg-Brentano XRD uklon Rentgen žarkov, Rutherford sipanje povratno, RBS spekter Rutherford sipanja povratnega, AES Auger Spektroskopija elektronska - profiliranje globinsko, Ni-Si razmerje sestavin povprečno, faze difuzije medsebojne, kontaminacija s kisikom

Povzetek: S sprotnim merjenjem električne upornosti med segrevanjem s stalno hitrostjo 3°C/min do 500°C ter s kasnejšimi meritvami rentgenskega uklona, Rutherfordovega povratnega sipanja ter spektrov Augerjevih elektronov smo sistematično študirali mešanje plasti niklja in silicija v različnih dvoplastnih ter večplastnih zgradbah s povprečno sestavo med $Ni_{0.78}Si_{0.22}$ in $Ni_{0.28}Si_{0.72}$. Zaporedje nastajanja faz je odvisno od razmerja začetnih debelin obeh elementov. V večplasteh smo zaznali difuzijo že nad 150°C. Dodatno smo opazovali tudi dvoplasti z različno vsebnostjo kisika v posameznih plasteh. Nekaj odstotkov vgrajenega kisika v plasti močno omeji medsebojno difuzijo.

1. Introduction

Silicides have been a subject of research for many years. Their attractiveness has certainly been triggered by the characteristics of the metal/Si reaction, which have made the metal/Si diffusion couple a standard research subject for thin film reactions /1,2/. The sequence of the formation of phases from metal and silicon layers during heat treatment has only been established in a few silicide systems. Perhaps the most extensively studied of these is the Ni-Si system /3/. The potential microelectronics applications have widened the scope of research and have brought new characterization methods. Among other methods in-situ electrical resistivity measurement /4,5/ has been used to characterize interactions in Ni-Si system. However, these results have been obtained on two different structures only. In this paper we present a systematic analysis of reactions in different structures made of Ni and Si layers.

2. Experiment

Structures to be analyzed were deposited as 2.5 mm wide and 8 mm long strip onto polished (Ra = 25 nm) ceramic alumina substrates between two previously printed and annealed (at 850°C) thick film golden contacts which were bonded to the pads on a ceramic sample holder to enable the in-situ electrical resistivity measurement /6,7/. The sample was connected in series with a large resistor to the lock-in amplifier which measured the voltage drop on a film during heat treat-

Table 1: Description of the as deposited state of various types of films used in this study

sample type	Charge No.	No. of layers	d_A (nm)	d_B (nm)	A	B	overall stoichiometry	R_{RT} (Ohm)
A	1361	2	53	27	Ni	Si	$Ni_{0.78}Si_{0.22}$	14.8
B	1362	2	53	55	Ni	Si	$Ni_{0.64}Si_{0.36}$	14.2
C	1363	2	53	82	Ni	Si	$Ni_{0.54}Si_{0.46}$	12.6
D	1310	2	53	91	Ni	Si	$Ni_{0.52}Si_{0.48}$	14.4
E	1311	2	53	157	Ni	Si	$Ni_{0.38}Si_{0.62}$	15.2
F	1367	2	53	75	Ni	Si+O		14.3
G	1309	2	53	53	Ni	Si+O		17.2
H	1364	2	53	55	Ni	Si+O		15.1
I	1366	2	52	55	Ni+O	Si+O		68
J	1365	2	68	55	Ni+O	Si+O		560
K	1300	2	200	152	Ni	Si	$Ni_{0.71}Si_{0.29}$	4.1
L	1256	11	25	30	Ni	Si	$Ni_{0.56}Si_{0.44}$	4.9
M	1259	11	25	95	Ni	Si	$Ni_{0.28}Si_{0.72}$	5.1

ment. The resistivity of the film was typically four orders of magnitude lower than that of the resistor.

Silicon and nickel layers were sputtered in a RF mode at a power of 1000 W and in a DC mode at 1700 V / 0.6A, respectively, at the argon pressure of 0.2 Pa. During the deposition substrates were covered by masks to form strips of the measured film. In the as-deposited state transmission electron microscopy revealed that Si layers were amorphous and Ni layers were fine-grained polycrystalline with an average grain size of 20 nm.

As deposited samples were inserted into a tube furnace with argon or nitrogen gas flow at the atmospheric pressure. The temperature of the sample was monitored by a thermocouple levitating above it. The furnace was heated up at a constant rate of 3°C/min in all experiments and the resistivity was measured continuously in situ through the bonded contacts.

Measurements were done on various bilayers and multilayer samples with alternating Si and Ni layers of different thicknesses (Table 1). Some samples were contaminated with oxygen during deposition by inletting oxygen gas into the chamber.

Bilayers and multilayers of all groups were first heated at constant rate of 3°C/min while resistivity was continuously measured *in-situ*. After the determination of interesting temperatures, samples with the same structures deposited onto a silicon wafer with grown native oxide layer (Si monocrystal for easier X-ray spectral analysis and oxide layer to prevent from film-substrate interaction) were heated in the same way, but were taken out of the furnace at such temperature values to be later (*ex-situ*) analyzed by other techniques. On cooled samples X-ray diffraction (XRD) (Huber G600 diffractometer with Seemann-Bohlin (SB) geometry or Philips PW1710 diffractometer with Bragg-Brentano (BB) geometry), Rutherford backscattering spectro-metry (RBS) (Van de Graaff accelerator) and Auger electron spectroscopy (AES) sputter depth profiling (PHI 545A scanning Auger microprobe) were done to be compared with the results of the resistivity measurement. In x-ray diffraction of thin films classical Bragg-Brentano geometry (Read camera) /8/ is used for oriented samples with crystall planes parallel with the surface while Seemann-Bohlin geometry is best suited for randomly oriented polycrystalline samples.

3. Results and discussion

Results of the in-situ electrical resistivity measurement of bilayer types A, B, C, D, E and K during heating are presented in Figure 1.

It can be seen that in all those samples there is an influence of the temperature coefficient of a resistivity at low temperatures which is followed by an increase which is more pronounced for bilayers with thicker Si

layer. The behaviour at higher temperatures depends on Si content as well. In curves A and B and K the increase is temporarily interupted by a decrease, continues again and becomes saturated. In curves D and E with the highest Si/Ni thickness ratio the increase is followed by an even more abrupt drop which later saturates at lower values. The curve C represents an intermediate case.

Samples of groups A, B, C, D and E with the same Ni thickness of 53 nm exhibit almost the same resistivity behaviour at low temperatures in Figure 1. At 260°C their resistivity already deviates from a linear increase. Rutherford backscattering spectra (RBS) in Figure 2 reveals that this is due to the interaction between both layers as the right edge of Ni signal and the left edge of Si signal are changed at this temperature in comparison with the as-deposited state. During the exponential increase of the resistivity both Ni and Si layers are being consumed while new intermediate silicide layer is growing. The overall conductivity of the bilayer is mostly determined by parallel resistivities of Ni and silicide layers. The consumed nickel appears in the form of the silicide which exhibits larger specific electrical resistivity than the pure metal. Therefore the resistivity is increasing as the silicide layer is growing at the interface.

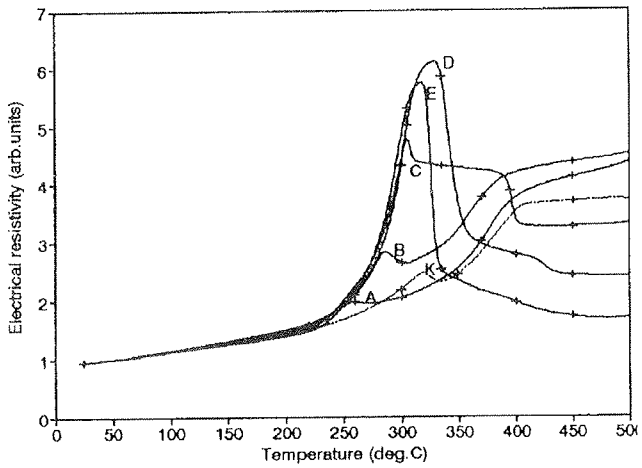

Figure 1: In-situ temperature dependence of electrical resistivity for bilayers with Ni and Si thicknesses of 53 nm/27 nm (A), 53 nm/55 nm (B), 53 nm/82 nm (C), 53 nm/91 nm (D), 53 nm/157 nm (E) and 200 nm/152 nm (K), respectively, heated up at 3°C/min in argon. Crosses mark temperatures to which XRD and RBS measurements correspond.

RBS of the sample A in Figure 2 shows that resistivity increase between 220 and 260°C can be attributed to the interdiffusion at the interface between both layers which consumes all Si layer below 260°C. This diffusion is then temporarily limited between 260 and 300°C where resistivity exhibits a peak, probably due to a crystallization of Ni_2Si like it will be later shown for sample B. Next Ni diffusion into the silicide is taking place which is becoming slower as the depth distribution of nickel is becoming more homogenous.

In the sample B thicker Si layer is consumed at higher temperature (below 300°C) than for the sample A as can be seen in Figure 2. The resistivity of the sample drops slightly and then rises again up to the saturated value. The drop corresponds to the crystallization of Ni_2Si as its peaks appear in the XRD spectrum at 300°C (Figure 3). According to RBS spectra crystallization of the newly-formed silicide can start only after the limitatation of the diffusion. The following resistivity rise is due to the diffusion of Ni into the silicide layer (and therefore Ni layer consumption). The ending silicide stoichiometry is defined by the starting content of both elements in a bilayer. XRD spectra indicate that between 370 and 450°C recrystallization is taking place yielding a mixture of Ni_2Si and $Ni_{31}Si_{12}$.

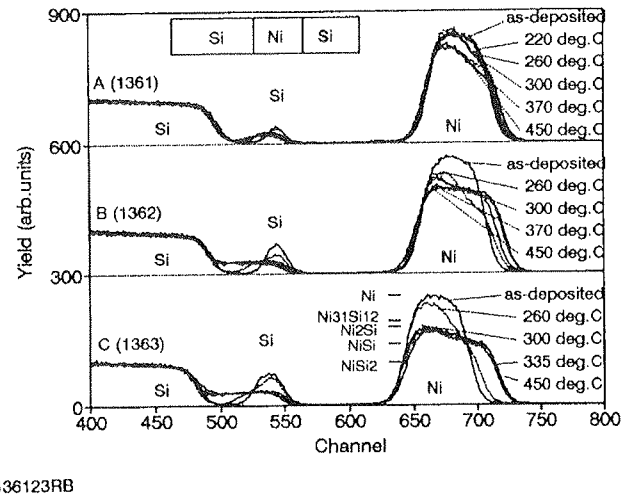

Figure 2: Ex-situ 1.45 MeV $^4He^+$ Rutherford backscattering spectra of samples A, B and C with Ni and Si thicknesses of 53 nm/27 nm, 53 nm/55 nm and 53 nm/82 nm, respectively, heated at 3°C/min. up to different temperatures in argon and then cooled rapidly. The signal of Ni layer appears at higher channels (ener-gies) than the signal of Si layer due to larger mass of Ni atoms in comparison with Si atoms although Ni layer is located below Si layer.

The sample C, exhibits strong initial increase. Here the difference between RBS spectra (Figure 2) obtained at room temperature, 260 and 300 °C is easy to notice. The intermixing in samples A, B and C is more rapid for thicker Si layers as Si atoms seem to diffuse more rapidly than do the Ni atoms. In X-ray diffraction spectrum of the sample C (Figure 4) at 300°C only broad and weak Ni peak is present which seems to get a neighbour of the growing Ni_2Si phase. Namely, at 335°C peaks of this new phase appears. Obviously resistivity detects

well the consumption of initial layers and the crystallization of Ni_2Si. Moreover, while RBS spectra remain almost constant above 335°C in Figure 2, the resistivity of the sample C in Figure 1 drops obviously around 395°C and this agrees well again with XRD spectra in Figure 4 where additional peak of the NiSi phase appears at 395°C which is more pronounced at 450°C.

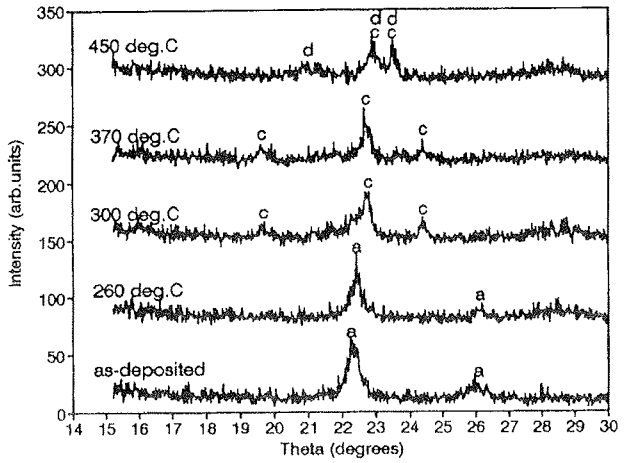

Figure 3: Ex-situ Seemann-Bohlin x-ray diffraction (XRD) spectra of the sample B (53 nm Ni/55 nm Si) after deposition and after heating at 3°C/min up to different temperatures and then cooled rapidly.

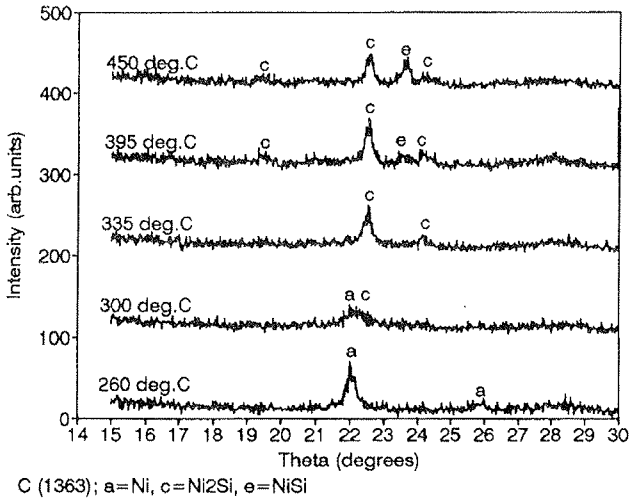

Figure 4: Ex-situ Seemann-Bohlin x-ray diffraction (XRD) spectra of the sample C (53 nm Ni/82 nm Si) after deposition and after heating at 3°C/min up to different temperatures and then cooled rapidly.

At this point it shall be explained that the sequence of the phases formed depends on the starting Ni/Si thickness ratio. The formation of nickel silicide between a film and a Si wafer exhibits a sequential growth of three phases: Ni_2Si, NiSi and $NiSi_2$ /9/. In a bilayer where Si layer is thinner than Ni layer Canali /10/ found different sequence: Ni_2Si, $Ni_{31}Si_{12}$ and Ni_3Si. Tu /11/ added this result to his results obtained on bilayers with thicker Si layer than Ni layer and suggested phase formation sequences for both cases: If Si layer is thinner than Ni layer Ni_2Si, $Ni_{31}Si_{12}$ and Ni_3Si will form sequentially. On the other hand if Si layer is thicker than Ni layer Ni_2Si, NiSi and $NiSi_2$ will appear with increasing temperature. It shall be noted here that references /10,11/ talk about Ni_5Si_2 as the existence of such phase was earlier reported by Saini /12/ and included with its characteristic peaks into reference x-ray diffraction pattern /13/. Later a correction of the stoichiometry to $Ni_{31}Si_{12}$ was included into this pattern /14/.

Samples D and E with high silicon content, like the sample C, exhibit strong initial resistivity increase. XRD spectra in Figures 5 and 6 show that the resistivity drop after the already explained increase (Figure 1) can again be correlated well with the crystallization of the NiSi phase as for the sample C. As can be seen in Figure 1 this process appears at lower temperatures for films with thicker initial Si films. It is interesting that peaks of both Ni_2Si and NiSi appear in the same temperature range between 305 and 335°C which differs from the sample C where peaks of only Ni_2Si appeared first and those of NiSi were added later. This may be caused by a Si diffusion which is rapid in comparison with sample A. However, RBS spectra of the sample E in Figure 7 reveal that after quite homogenous silicide layer with a stoichiometry close to NiSi is formed, the diffusion of remaining Si layer is limited. Evidently even temperature of 450°C is not high enough to enable the formation of homogenous layer with higher silicon content (e.g. $NiSi_2$).

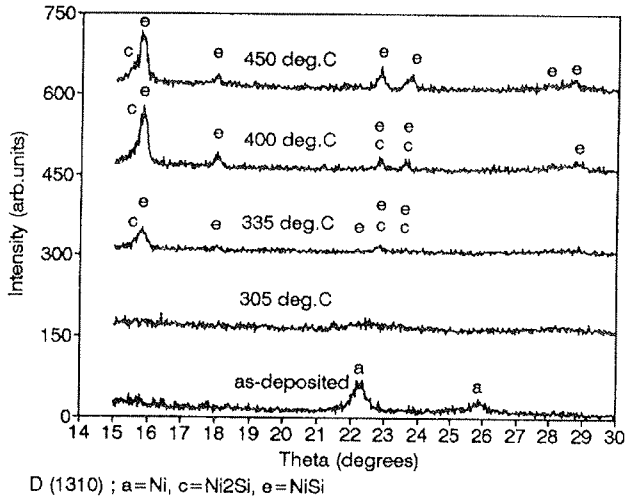

Figure 5: Ex-situ Seemann-Bohlin x-ray diffraction (XRD) spectra of the sample D (53 nm Ni/91 nm Si) after deposition and after heating at 3°C/min up to different temperatures and then cooled rapidly.

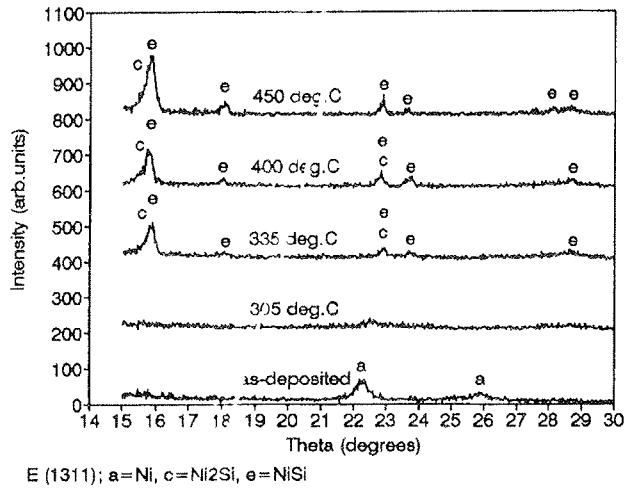

Figure 6: Ex-situ Seemann-Bohlin x-ray diffraction (XRD) spectra of the sample E (53 nm Ni/157 nm Si) after deposition and after heating at 3°C/min up to different temperatures and then cooled rapidly.

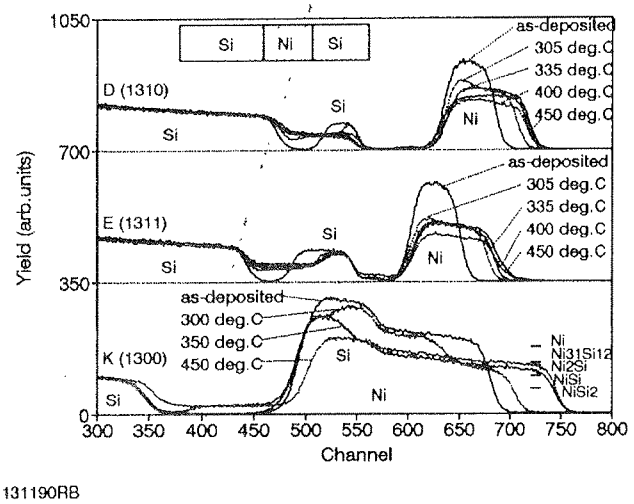

Figure 7: Ex-situ 1.45 MeV $^4He^+$ Rutherford backscattering spectra of samples D, E and K with Ni and Si thicknesses of 53nm/91nm, 53nm/157nm and 200nm/152nm, respectively, heated at 3°C/min. up to different temperatures in argon and then cooled rapidly.

Up to this point bilayers with the same thickness of Ni layer were presented. This was done to enable the comparison between different bilayers with various thicknesses of Si layer as initial resistivity is determined mostly by nickel. Now we shall examine the effect of thicker Ni layer in the sample K. Its resistivity dependence is similar to that of the sample B which possesses similar starting Ni/Si thickness ratio. The resistivity curve K in Figure 1 is shifted to higher temperatures as it can be expected that it takes more time for thicker layer of Ni to be consumed during temperature ramp. A comparison between XRD spectra in Figure 3 (sample B) and Figure 8 (sample K) shows that in both cases at temperatures below the resistivity peak traces of Ni are present only. Above the peak beside traces of remaining Ni other peaks are present as well. In the case of sample K beside Ni_2Si peaks, visible in spectra of sample B, signs of $Ni_{31}Si_{12}$ and NiSi are present, too. It is possible that last two phases are also present in thinner bilayer samples with similar thickness ratio, but their quantities may be below the detection limit for XRD which is about 20 nm /11,16/. Another possibility is that higher temperatures needed in thicker bilayers for one of the layers to be consumed have effect on a process of the crystallization of the silicide layer which is triggered by this consumption. A presence of Ni_2Si, $Ni_{31}Si_{12}$ and NiSi in the sample K heated up to 350°C was noticed in XRD spectrum obtained in Bragg-Brentano geometry as well.

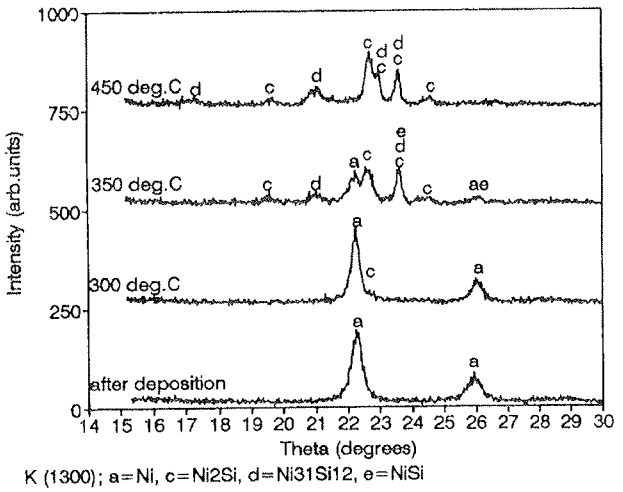

Figure 8: Ex-situ Seemann-Bohlin x-ray diffraction (XRD) spectra of the sample K (200 nm Ni/152 nm Si) after deposition and after heating at 3°C/min up to different tempera-tures and then cooled rapidly.

The sample K is thicker than other samples and signals from Ni and Si layers partially overlap in RBS spectra. At the same time larger thickness makes the observation of changes in depth profiles easier. At 300°C we can see that nickel atoms are detected at higher channels than after deposition - they are moving into the silicon layer, producing a step in a Ni signal which means that the growing silicide layer is rather homogenous. We analyzed RBS spectra by two different computer programs /17,18/ and found that the stoichiometry is between Ni_2Si and NiSi. At 350°C, after the resistivity peak, Ni atoms spread all the way to the surface of the film - all Si layer is consumed. Another evidence for this is smaller height of the right shoulder of Si signal. The second rise of the signal is due to remaining pure Ni layer near the substrate. The silicide layer exhibits stoichiometry close to Ni_3Si_2 which can be a mixture of Ni_2Si and NiSi as it was already observed in similar films /19/. If we heat the sample higher up to 450°C, Ni atoms

diffuse into the silicide and result in a homogenous film on a substrate. Its composition is defined by the starting overall composition of the bilayer. Nickel is not reacting with the substrate up to 450°C as can be seen from a non-moveable left edge of the Ni signal of other bilayer samples. The main reason for this comes from native oxide as oxides are known to limit interactions between films /20/.

To compare situation in samples A, B, C, D, E and K after heating at 3°C/min up to 450°C their x-ray diffraction spectra are presented in Figure 9. It can be clearly seen that situation depends on starting Ni/Si thickness ratio as well as on absolute values of thicknesses. For sample A nickel peak is the strongest and beside it small peaks of Ni_2Si and $Ni_{31}Si_{12}$ appear. If we increase the thickness of silicon, nickel peaks disappear and only peaks belonging to other two phases remain in sample B. Sample C possesses no traces of $Ni_{31}Si_{12}$. Instead, NiSi peak grows up beside peaks of Ni_2Si. If we increase Si content furter, peaks of NiSi become dominant. As Si layer is amorphous we do not detect it although there is some remaining Si layer in sample E. Situation in sample K is similar to the state of sample B except the number of phases detected is larger.

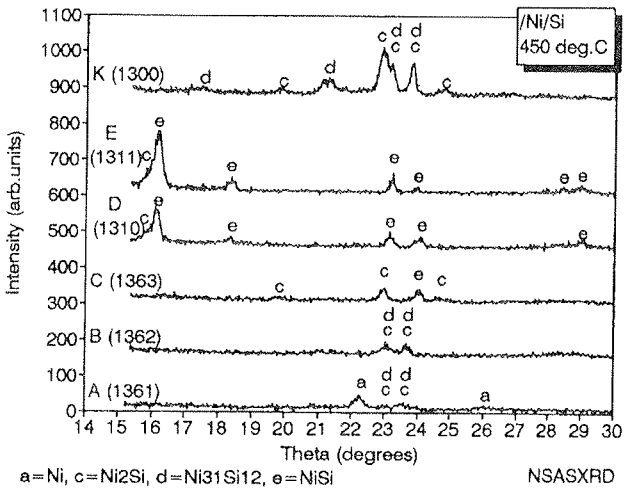

Figure 9: Ex-situ Seemann-Bohlin x-ray diffraction (XRD) spectra of bilayers with Ni and Si thicknesses of 53nm/27nm (A), 53 nm/55 nm (B), 53nm/82 nm (C), 53nm/ 91nm (D), 53nm/ 157nm (E) and 200nm/152nm (K), respectively, heated up to 450°C at 3°C/min in argon and then cooled rapidly.

As can be seen in Table 1 several samples were contaminated with oxygen during deposition to study its influence on interactions between nickel and silicon. Depth profiles of samples F, G, H, I and J are presented in Figure 10. As AES is not an absolute analytical method several standards would be needed to calibrate these measurements. Therefore, Auger peak-to-peak height is used for presentation which enables relative comparison of similar samples. We applied RBS method which is absolute, too. It is not best suited for light elements, but as an estimation it gives the stoichiometry of SiO_2 in oxidized Si layer of the sample F and $Ni_{0.8}O_{0.2}$ in oxidized Ni layer of the sample J.

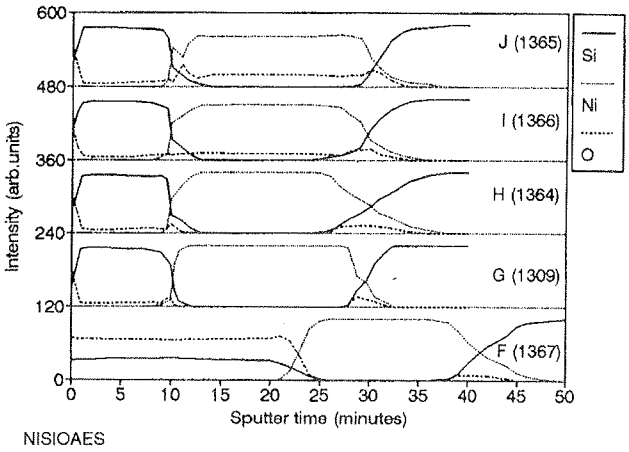

Figure 10: Auger electron spectroscopy (AES) depth profiles of as-deposited bilayer samples F, G, H, I and J, contaminated with oxygen during deposition.

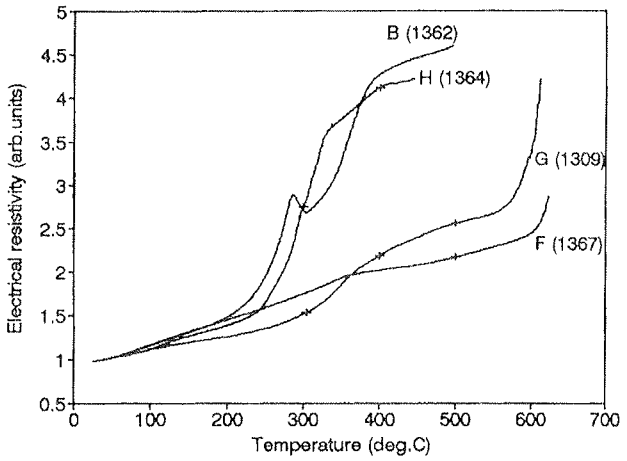

Figure 11: In-situ temperature dependence of electrical resistivity for bilayers without oxygen contamination (type B) and with oxygen included into Si layers (types F, G and H with decreasing oxygen content) heated up at 3°C/min in argon and then cooled rapidly. Crosses mark points to which RBS and XRD measurements correspond.

As can be expected /20/ oxygen limits interactions. In-situ dependence of resistivity for samples with contaminated Si layers is given in Figure 11. Resistivity dependence of sample B which was not intentionally contaminated is shown for reference. It can be seen

clearly that several per cent of incorporated oxygen can strongly limit interactions in sample G. In sample F, where SiO_2 was grown on Ni, we can see the Currie point of nickel at 260°C - resistivity dependence similar to one we get if nickel is deposited only. There is good correlation between resistivity measurements in Figure 11 and RBS spectra in Figure 12. The lesser the changes in resistivity the more constant RBS signal is. X-ray diffraction spectra of those samples in Figure 13 heated up to 400°C or more confirms observations of both techniques that the formation of new phases is strongly suppressed if oxygen is present.

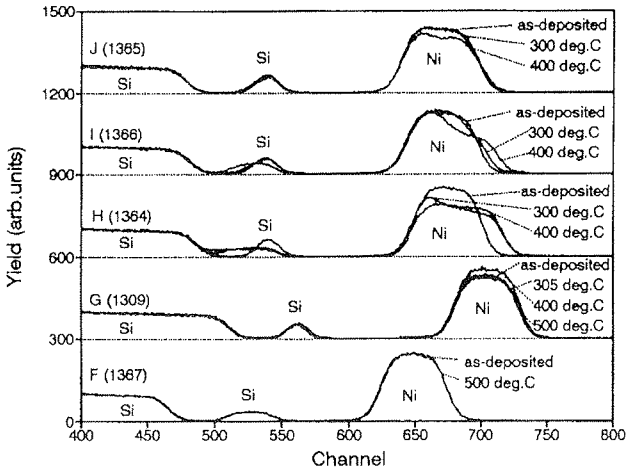

Figure 12: Ex-situ $^4He^+$ Rutherford backscattering spectra for bilayers without oxygen contamination (type B), with oxygen included into Si layers (types F, G and H with decreasing oxygen content) and with oxygen included into Ni layers (types I and J with increasing oxygen content) heated up to different temperatures at 3°C/min in argon and then cooled rapidly. The energy of the incoming ions was 1.45 MeV (F, H, I and J) and 1.5 MeV (G).

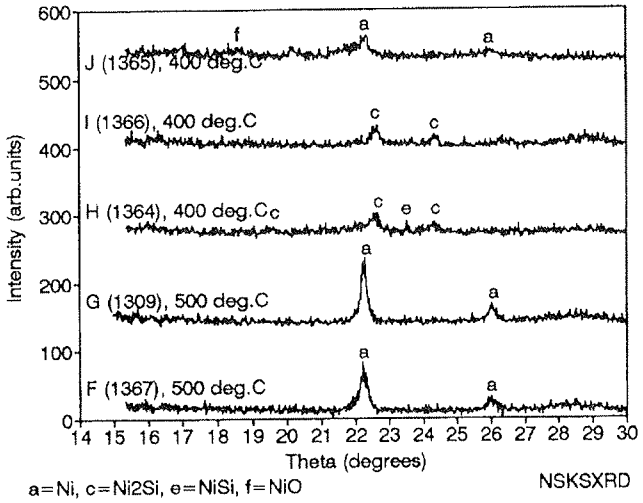

Figure 13: Ex-situ Seemann-Bohlin x-ray diffraction (XRD) spectra of bilayer samples F, G, H, I and J, contaminated with various amounts of oxygen during deposition, heated up to 400 or 500°C at 3°C/min in argon and then cooled rapidly.

If silicon layer is contaminated, mostly conducting nickel layer is unaffected. Resistivity measurements can be normalized with room temperature values and compared mutualy. On the other side if nickel layer is contaminated its resistivity can be increased by orders of magnitude. Therefore, in such samples absolute values of resistivity are to be compared as is presented in Figure 14. Their resistivity during heating alters and some changes can be seen in RBS spectra in figure 12 as well. Additionally, the state of samples I and J at 400°C is described by their XRD spectra in Figure 13.

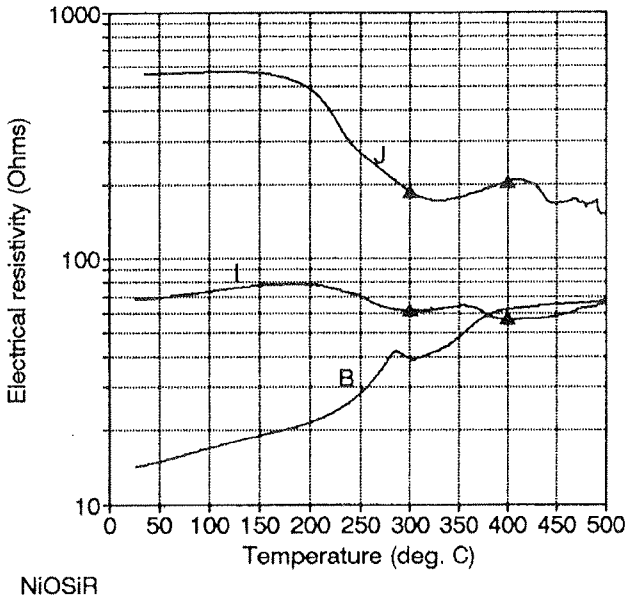

Figure 14: In-situ temperature dependence of electrical resistivity for bilayers without oxygen contamination (type B) and with oxygen included into Ni layers (types I and J with increasing oxygen content) heated up at 3°C/min in argon and then cooled rapidly. Triangles mark points to which RBS and XRD measurements correspond.

After the analysis of results on bilayers we shall focus on multilayer structures, containing 11 alternating layers of nickel and silicon. Multilayer samples from the group L have Si and Ni layer thicknesses of 30 and 25 nm, respectively. Group M possesses Si and Ni layer thicknesses of 95 and 25 nm, respectively. Taking into account the different volume density of atoms of the two elements, the Si/Ni ratio of the total number of atoms in a multilayer was 0.8 and 2.1 for group A and B, respectively. Obtained resistivity dependencies on temperature, along with results for bilayers C and E possessing similar overall stoichiometries, are shown in Figure 15.

Crosses again mark points to which x-ray diffraction spectra for the group L and M in Figure 16 and Figure 17, respectively, correspond.

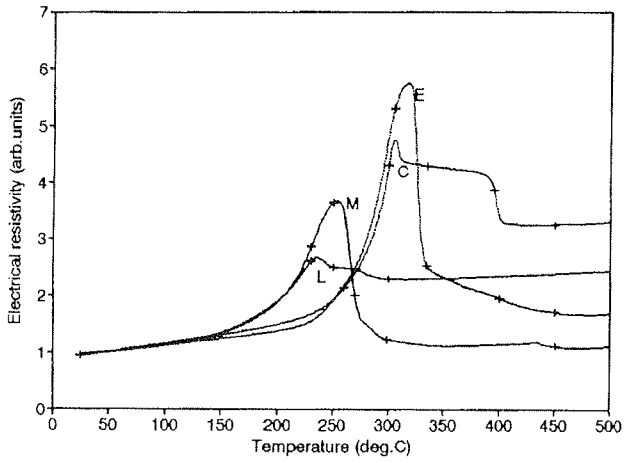

Figure 15: In-situ temperature dependence of electrical resistivity for bilayers with Ni and Si thicknesses of 53 nm/82 nm (C) and 53 nm/ 157 nm (E) and for multilayers (11 alternating layers) with Ni and Si individual layer thicknesses of 25 nm/30 nm (L) and 25 nm/95 nm (M), respectively, heated up at 3°C/min in argon. Crosses mark tempera-tures to which XRD and RBS measurements correspond.

As in bilayers temperatures of similar resistivity change were lower for the sample B than for the sample K, in multilayers composed of even thinner layers these temperatures are lower than for bilayers. The curves for bilayers and multilayers are, however, similar.This can be seen in figure 15. The expectance that similar resistivity behaviour describes processes like those in bilayers is confirmed by x-ray diffraction in Figure 16, where for the sample L the crystallization of Ni_2Si phase above resistivity peak was detected. After their appearance, at higher temperatures these peaks are shifting toward higher angles - the crystals are ordering and unit cells are becoming smaller. In sample M peaks of Ni_2Si are detected in the diffraction spectrum at the resistivity peak (Figure 17) and the following resistivity drop is connected with the appearance of crystalline NiSi beside still existing Ni_2Si. Finally, at 450°C NiSi phase is detected only by x-ray diffraction. In general for multilayer sample M reactions are similar to those in bilayer sample E. There are, however, differences in details. XRD spectra for bilayers in Bragg-Brentano geometry yield up to four times higher signals than in Seemann-Bohlin geometry while in multilayers the ratio of even 100 was noticed. This indicates that the crystallization in multilayers yields more oriented structures than in bilayers. Another difference is that in diffraction spectrum of multilayer M peaks of Ni_2Si are much more obvious than in bilayer E (and peaks of NiSi much less dominant) although the silicon content in the multilayer is higher than in the bilayer. RBS measurements in Figure 18 reveal that multilayer structure in sample L is ruined at 250°C yielding a homogenous depth profile. On the other hand, in multilayer M the alternating structure is affected but still visible even at 450°C. The reason for this may be similar as in bilayer E, where the intermixing is limited after a stoichiometry close to NiSi is obtained in a newly formed silicide layer.

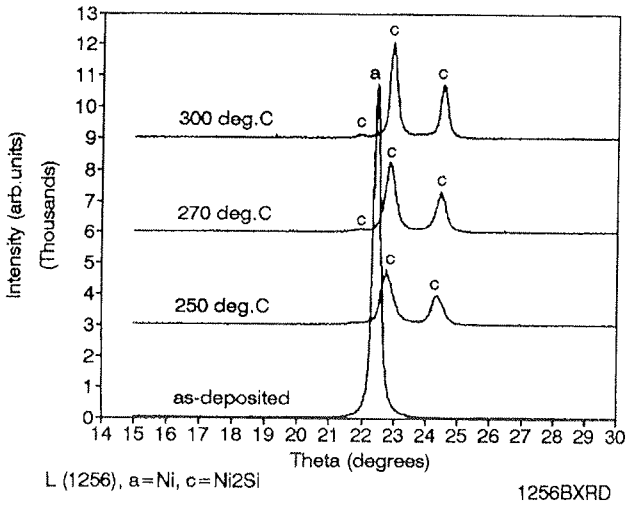

Figure 16: Ex-situ Bragg-Brentano x-ray diffraction (XRD) spectra of the sample L (11 alternating layers; 25 nm Ni, 30 nm Si) after deposition and after heating at 3°C/min up to different temperatures and then cooled rapidly.

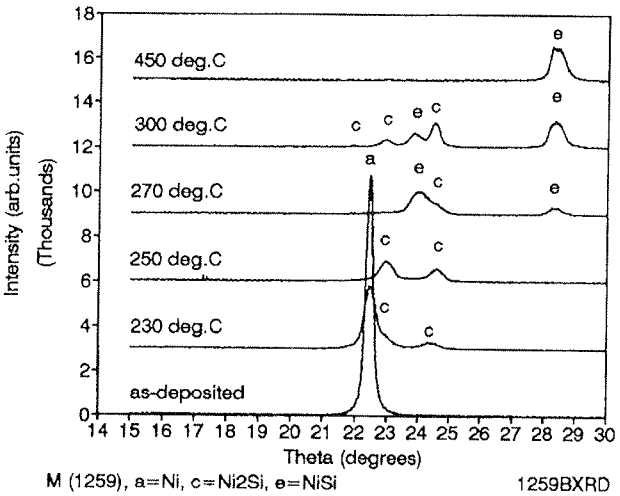

Figure 17: Ex-situ Bragg-Brentano x-ray diffraction (XRD) spectra of the sample M (11 alternating layers; 25 nm Ni, 95 nm Si) after deposition and after heating at 3°C/min up to different temperatures and then cooled rapidly.

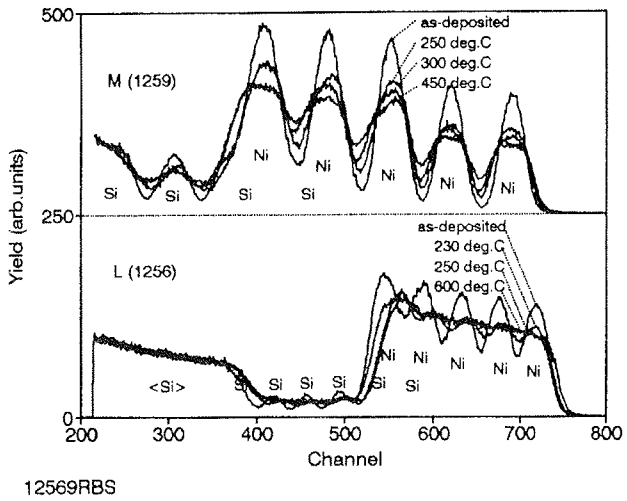

Figure 18: Ex-situ 1.5 MeV $^4He^+$ Rutherford backscattering spectra of multilayers (11 alternating layers) with Ni and Si individual layer thicknesses of 25 nm/30 nm (L) and 25nm/95nm (M), respectively, heated up at 3°C/min in argon.

4. Conclusions

We analyzed interaction between Ni and Si layers in bilayers and multilayers with various Ni/Si thicknnesses ratios on a basis of in-situ electrical resistivity measurements during dynamic heating of the sample. Results of resistivity curves prooved to be efficient starting points for straightforward use of other analytical methods as x-ray diffraction, Rutherford backscattering and Auger electron depth profiling and observations of all methods were well correlated. Temperatures at which phases occur after the intermixing of both elements depend on properties of measured structure.

In literature in the case of Ni on Si wafer Ni_2Si, NiSi and $NiSi_2$ were observed after an isothermal anneal at 280, 350 and 750 °C, respectively /11/. In bilayers with thinner Si layer Ni_2Si, $Ni_{31}Si_{12}$ and Ni_3Si were detected after similar heating at 280, 400 and 450 °C /10/. Several authors noticed Ni_2Si at 200 °C and $NiSi_2$ was found on amorphous silicon at 400°C /15/.

In our bilayers peaks of Ni_2Si were found in the sample B at 300°C, but according to RBS and resistivity measurements it is present already at 260°C. Additionaly it shall be noted that in multilayers with thinner layers resistivity exhibited changes about 50°C lower and similar temperature difference was found in XRD spectra as well. Presence of $Ni_{31}Si_{12}$ was noticed at 450°C in thinner bilayer B) and at 350°C in thicker bilayer (K). The formation temperature for NiSi in our bilayers depended on starting Ni/Si thickness ratio and varied between 335 and 395°C. In multilayers this temperature was again 50°C lower than the lowest temperature for bilayers. For temperatures up to 450°C $NiSi_2$ was firmly detected neither in bilayers nor in multilayers.

The incorporation of several atomic per cent of oxygen atoms into silicon or nickel layer suppresses the diffusion strongly. For lower oxygen contents Ni_2Si is present at 400°C, while for higher contents almost no changes are visible in x-ray diffraction and Rutherford backscattering spectra.

References

/1/ K. Maex, Materials Science and Engineering R11 (1993) 53.

/2/ M. Ohring, The Materials Science of Thin Films, Academic Press Inc., Boston, 1992, 389.

/3/ M. Ohring, The Materials Science of Thin Films, Academic Press Inc., Boston, 1992, 391.

/4/ Y. Kawazu, H. Kudo, S. Onari in T. Arai, Jap. J. Appl. Phys. 29 (1990) 729.

/5/ Q.Z. Hong, Stella Q. Hong, F.M. D'Heurle in J.M.E. Harper, Thin Solid Films 253 (1994) 479.

/6/ A. Cvelbar, B. Čuk, P. Panjan, B. Navinšek and A. Zalar, Vacuum 46 (1995) 923.

/7/ B. Navinšek, P. Panjan and A. Cvelbar, Surface and Coatings Technology 74-75 (1995) 155.

/8/ L.C. Feldman and J.W. Mayer, Fundamentals of Surface and Thin Film Analysis, North-Holland, New York, 1986, p. 168.

/9/ J.M.Poate, K.N.Tu and J.W. Mayer, Eds.: Thin Films - Interdiffusion and reactions, John Wiley & Sons, New York, 1978, p. 368.

/10/ C. Canali, G. Majni, G. Ottaviani in G. Celotti, J. Appl. Phys. 50 (1979) 255.

/11/ K.N.Tu, G. Ottaviani, U. Gösele in H. Föll, J. Appl. Phys. 54 (1983) 758.

/12/ Saini et al., Can. J. Chem. 42 (1964) 1511.

/13/ ASTM Card 17-222.

/14/ Powder Diffraction File 17-222, Joint Committee of Powder Diffraction Standard International Centre of Diffraction Data, New Town, 1994.

/15/ R. Pretorius, T.K. Marais and C.C. Theron, Materials Science and Engineering 10 (1993) 1.

/16/ J.M. Poate, K.N.Tu and J.W. Mayer, Eds.: Thin Films - Interdiffusion and reactions, John Wiley & Sons, New York, 1978, p.365.

/17/ E. Kotai, Nucl. Instr. Meth. B 92 (1994) 100.

/18/ J. Saarilahti and E. Rauhala Nucl. Instr. Meth. B 64 (1992) 734.

/19/ A. Zalar, S. Hofmann, F. Pimentel and P. Panjan, Surf. and Interf.Analysis 21 (1994) 560.

/20/ C.-D. Lien and M.-A. Nicolet, J. Vac. Sci.Technol. B 2 (1984) 738.

Mag. Andrej Cvelbar, dipl.ing.
Dr. Peter Panjan, dipl.ing.
Prof. Dr. Boris Navinšek, dipl.ing.
Benjamin Zorko, dipl.ing.
Doc.Dr.Miloš Budnar, dipl.ing.
Institut "Jožef Stefan"
Jamova 39, 61000 Ljubljana, Slovenia
tel: +386 61 177 3900
FAX: +386 61 219 385

Doc. Dr. Anton Zalar, dipl.ing.
Borut Praček, dipl.ing.
Institut za elektroniko in vakuumsko tehniko
Teslova 30, 61000 Ljubljana, Slovenia
tel: +386 61 126 4584
FAX: +386 61 263 098

Prispelo (Arrived): 03.10.95 *Sprejeto (Accepted): 17.10.95*